Author Manuscript

Author Manuscript

Author Manuscript

Author Manuscript

HHS Public Access

Author manuscript

J Neurogenet. Author manuscript; available in PMC 2018 December 01.

Published in final edited form as:

J Neurogenet. 2017 December ; 31(4): 325–336. doi:10.1080/01677063.2017.1393076.

Generation and Characterization of New Alleles of *quiver* (*qvr*) That Encodes an Extracellular Modulator of the Shaker Potassium Channel

Hongyu Ruan[a,@,*], **Atsushi Ueda**[a,*], **Xiaomin Xing**[a,*], **Xuxuan Wan**[a,@@], **Benjamin Strub**[b], **Spencer Mukai**[b], **Kaan Certel**[c,@@@], **David Green**[a,@@@@], **Kyle Belozerov**[b], **Wei-Dong Yao**[a,@], **Wayne Johnson**[c], **Jim Jung-Ching Lin**[a], **Arthur J. Hilliker**[b], and **Chun-Fang Wu**[a,†]

[a]Department of Biology, University of Iowa, Iowa City, IA, USA, 52242

[b]Department of Biology, York University, Toronto, ON, M3J 1P3, Canada

[c]Department of Molecular Physiology and Biophysics, University of Iowa, Iowa City, IA, USA, 52242

Abstract

Our earlier genetic screen uncovered a paraquat-sensitive leg-shaking mutant *quiver*^{1} (*qvr*^{1}), whose gene product interacts with the *Shaker* (*Sh*) K^+ channel (Humphreys et al, 1996; Wang et al., 2000). We also mapped the *qvr* locus to EY04063 and noticed altered day-night activity patterns in these mutants. Such circadian behavioral defects were independently reported by another group, who employed the *qvr*^{1} allele we supplied them, and attributed the extreme restless phenotype of EY04063 to the *qvr* gene. However, their report adopted a new noncanonical gene name *sleepless* (*sss*) for *qvr* (Koh et al., 2008). In addition to *qvr*^{1} and *qvr*^{EY}, our continuous effort since the early 2000s generated a number of novel recessive *qvr* alleles, including EMS-induced mutations *qvr*^{2} and *qvr*^{3}, and P-element excision lines *qvr*^{ip6} (imprecise jumpout), *qvr*^{rv7} and *qvr*^{rv9} (revertants) derived from *qvr*^{EY}. Distinct from the original intron-located *qvr*^{1} allele that generates abnormal-sized mRNAs, *qvr*^{2} and *qvr*^{3} had their lesion sites in exons 6 and 7, respectively, producing nearly normal-sized mRNA products. A set of RNA-editing sites are nearby the lesion sites of *qvr*^{3} and *qvr*^{EY} on exon 7. Except for the revertants, all *qvr* alleles display a clear ether-induced leg-shaking phenotype just like *Sh*, and weakened climbing abilities to varying degrees. Unlike *Sh*, all shaking *qvr* alleles (except for *qvr*^{f01257}) displayed a unique activity-dependent enhancement in excitatory junction potentials (EJPs) at larval neuromuscular junctions (NMJs) at very low stimulus frequencies, with *qvr*^{EY} displaying the largest EJP and more significant NMJ overgrowth than other alleles. Our detailed characterization of a collection of *qvr* alleles help establish links between novel molecular lesions and different behavioral and physiological consequences, revealing how modifications of the *qvr* gene lead to a wide spectrum

†Corresponding author. chun-fang-wu@uiowa.edu. Phone: 319-335-1090.
@Present Address: Department of Psychiatry, SUNY Upstate Medical University
@@Present Address: China Medical Educational International Holding Co., Ltd, Shanghai, China
@@@Present Address: Strategy and Business Development at Sanofi, 640 Memorial Dr., Cambridge, MA, USA, 02139
@@@@Present Address: Dart Neuroscience, LLC, 12278 Scripps Summit Dr., San Diego, CA, USA, 92131
*These authors contribute equally to the study.

Author Manuscript Author Manuscript Author Manuscript Author Manuscript

of phenotypes, including neuromuscular hyperexcitability, defective motor ability and activity-rest cycles.

Keywords

Qvr/SSS; *Shaker*; *sleepless*; RNA editing; Ly-6/neurotoxin superfamily; synaptic plasticity; potassium current inactivation; ether-induced leg shaking

Introduction

The original *Drosophila quiver* (*qvr*) allele qvr^1 was isolated in a screen for mutants with hypersensitivity to paraquat, an herbicide that generates reactive oxygen species (ROS) in living organisms. It was named *qvr* as the mutant flies exhibited a leg-shaking phenotype under ether anesthesia (Humphreys et al., 1996), resembling what was found in the canonical K^+ channel mutant *Shaker* (*Sh,* Kaplan and Trout, 1969; Jan et al., 1977). Therefore, our follow-up study focused on the electrophysiological characterization of *qvr* (Wang, 1997; Wang et al., 2000; Wang and Wu, 2010), and revealed that similar to *Sh*, *qvr* also specifically impaired fast-inactivating A-type K^+ current (I_A) (Salkoff and Wyman, 1981; Wu and Haugland, 1985) in larval body-wall muscles, without affecting other currents, such as delayed rectifier I_K (Singh and Singh, 1999; Hegde et al., 1999; Peng and Wu, 2007), Ca^{2+} current I_{Ca}, and Ca^{2+}-dependent K^+ current, fast I_{CF} and the slow I_{CS} (Elkins et al., 1986; Singh and Wu, 1989; Komatsu et al., 1990).

We independently mapped the *qvr* locus to EY04063 and studied its molecular lesions, larval and adult physiology, and double-mutant interaction with hyperexcitable K^+ channel mutants, as documented in a PhD thesis (Ruan, 2008) and conference presentations (Ueda et al., 2009; Wang et al., 2010; Wang and Wu, 2010; Xing et al., 2011). However, in the meantime, a report on similar molecular characterization and altered activity-rest cycles was published by another group, employing the original qvr^1 allele we provided to confirm that qvr^1 and EY04063 are allelic. The report nevertheless adopted a different gene name, *sleepless* (*sss*), (Koh et al., 2008), a departure from the standard fly community convention for gene naming, i.e. $qvr^{EY04063}$ instead of $sss^{EY04063}$. This and subsequent studies also reported that *qvr* encodes a glycophosphatidylinositol (GPI)-anchored small peptide (158 amino acids) belonging to Ly-6/neurotoxin superfamily (Tsetlin, 1999), which regulates Shaker's expression, localization and activity (Koh et al., 2008; Wu et al., 2010; Wu et al., 2014; Wu et al., 2016).

Based on an earlier dataset in the 1990's (Wang, 1997; Wang et al., 2000), a striking frequency-dependent enhancement in the postsynaptic excitatory junctional currents (EJCs) was found at neuromuscular junctions (NMJs) of qvr^1 larvae (Wang and Wu, 2010). This phenotype was associated with altered recovery from inactivation of the I_A current, which was uncovered in qvr^1 larval muscles to contain two distinct components: I_{AF} (fast recovery) and I_{AS} (slow recovery) (Wang, 1997; Wang and Wu, 2010). Later it was reported that dysfunction of C-type inactivation of the Shaker channel in the absence of Qvr results in the loss of I_{AS} current (Dean et al., 2011). Despite this significant progress, the limited variety

Author Manuscript Author Manuscript Author Manuscript Author Manuscript

of *qvr* mutant alleles restricts our perspective for understanding how Qvr contributes to a rich variety of neuromuscular excitability and behavioral phenotypes.

In this report, while clarifying the history of *qvr* discovery and characterization, we describe an array of unpublished *qvr* alleles with novel molecular lesions and physiological properties, summarizing the result of our continuous effort previously presented partly in thesis and meeting abstracts (Ruan, 2008; Ueda et al., 2009; Wang et al., 2010; Xing et al., 2011). qvr^{2} and qvr^{3} are point mutations, whereas qvr^{ip6}, qvr^{rv7} and qvr^{rv9} are excision lines generated from qvr^{EY}, displaying differed behavioral and electrophysiological properties. Together with qvr^{1}, qvr^{EY}, and another allele qvr^{f01257} (sss^{P2} in Koh et al., 2008), we characterized these new alleles molecularly, behaviorally, and electrophysiologically, so as to demonstrate the extent and diversity of *qvr* phenotypes and establish these mutant alleles for further investigation of *qvr*'s function in the control of neuromuscular excitability, synaptic transmission, and neural circuit function underlying day-night locomotive activities.

Materials and Methods

Fly stocks

Canton-S flies were used as the wild-type control. In addition to the point-mutation allele qvr^{1} (Humphreys et al., 1996), *cn* qvr^{2}, *cn* qvr^{3} were generated by EMS induction as described below. qvr^{EY} (also reported as $sleepless^{P1}$ by Koh et al., 2008) was derived after a background cleaning of the P element stock P{EPgy2}CG33472 (EY04063), which was ordered from the Bloomington stock center. qvr^{ip6}, qvr^{rv7} and qvr^{rv9} were derived by remobilizing the P element of qvr^{EY} (described below). Besides qvr^{EY}, we also independently identified PBac{WH}CG33472 (f01257) (Bloomington stock center, now renamed as PBac{WH}qvr^{f01257}) as an allele of *qvr* (reported as $sleepless^{P2}$, by Koh et al., 2008. In this study, it is referred to as qvr^{f01257}). All other P-element stocks used for deficiency mapping are listed in the supplementary materials. All flies were maintained at 22–23°C on standard fly food.

Ethyl methanesulfonate (EMS) mutagenesis

The protocol for treatment with EMS was adapted from the earlier work (Hilliker, 1976). 0–2 day old cn^{1} males were fed 0.025 M ethyl methanesulfonate (EMS) in 1% sucrose for 24 hours and then mated to qvr^{1}. Progeny exhibiting a *quiver* phenotype were identified and mated with bw^{V1}/*CyO-Sbw*, and the cinnibar-eye curly-wing progeny of this cross were interbred to create a stock. *cn* qvr^{2}, *cn* qvr^{3} were thus generated.

P-element remobilization and generation of new alleles

We remobilized the P-element by crossing EY04063 with a strain carrying P-element transposase (*y w;; Δ2-3, Sb/TM6, Ubx*). The leg-shaking phenotype was used to identify the imprecise excision lines by back crossing the excision lines to qvr^{1}. Individual lines were examined by genomic PCR to determine the nature of excision (Figure 3A). As expected, the precise excision lines, *ΔP-7*, *ΔP-8* and *ΔP-9*, no longer showed ether-induced leg-shaking and complemented with qvr^{1}; while the imprecise excisions behaved like *EY04063* (*ΔP-6*). To indicate the nature of the alleles, we renamed *ΔP-7*, *ΔP-8* and *ΔP-9* as qvr^{rv7}, qvr^{rv8},

Author Manuscript Author Manuscript Author Manuscript Author Manuscript

qvr^{rv9} ("rv" means "revertant"), and *ΔP6* as *qvr*^{ip6} ("ip" means "imprecise"). Therefore, the imprecise excision lines *qvr*^{ip6} represents new alleles of *qvr*.

Ether-induced leg shaking

A group of 20–30 flies were anesthetized in a chamber containing ether vapor for 3 to 5 seconds, and then placed on a tile for detecting leg shaking under a dissection microscope. A dissection microscope equipped with dark-field illumination was used to obtain photomicrographs of leg-shaking behaviors. Long-exposure (50 ms) images were captured by a commercially available regular digital camera (6 mega pixels per frame).

Fly climbing assay

Flies aged 4 days were collected and sexed into fresh vials, each containing 10 males or 10 females. Experiments were performed 4 days after the fly collection. Flies were transferred into clean plastic vials with foam plugs, and vortexed for 1 second. The number of flies that climbed above the midline of 4-cm height in 10 seconds was counted for each vial.

Genomic DNA extraction for sequencing

The insertion information of *qvr*^{EY} and *qvr*^{f01257} was obtained from the FlyBase (flybase.org). DNA sequencing was performed with *qvr*^{1}, *qvr*^{2}, and *qvr*^{3} to determine the lesion sites. To extract the genomic DNA, 25 homozygous male flies per strain were homogenized in 200 μl of homogenization buffer (0.1 M Tris, 0.1 M EDTA, 1.0% SDS, pH 9.5) in 1.5 ml polypropylene centrifuge tubes using a Teflon pestle and incubated at 70 °C for 20 min. Next, 28 μl of 8 M potassium acetate was added and the mixture was incubated for an additional 30 min on ice. The extract was centrifuged for 15 min at 16,000 xg at room temperature and then the supernatant was removed and diluted with 100 μl of sterile water to improve yield. DNA was extracted with phenol-chloroform, then precipitated from the aqueous phase with ethanol and washed with 70% ethanol, and finally the pellet was re-suspended in 100 μl of sterile water. Approximately 0.25 μg template DNA was used for PCR with the primers listed below. Forward: 5′-GCACGTTTTGGAATTCCTGT-3′; reverse: 5′-AGCCAAGATACTGCCACTGC-3′. The PCR product was used for sequencing.

Genomic DNA extraction and Polymerase chain reaction (PCR) for *qvr*^{EY} excision lines

Fifty young adult flies were collected and homogenized with 500 μl of solution A (0.1 M Tris-HCl, 0.1 M EDTA and 1% SDS, pH 9.0). After 30 min incubation at 70 °C, 70 μl of 8 M potassium acetate was mixed in the sample, which was then set on ice for 30 min and spun at 4 °C for 15 min. The supernatant was transferred to a new Eppendorf tube and 0.5 volumes of isopropanol were added. This mixture was then spun for 5 min and the resulting supernatant was removed, after which the pellet was re-suspended in 200 μl H_2O and an equal volume of phenol chloroform was added and mixed. The resulted mixture was then spun for another 5 min, and then the top aqueous layer was transferred to a new Eppendorf tube. 20 μl of sodium acetate and 440 μl of ice-cold ethanol was then added and mixed by inverting. The sample was next kept at -80 °C for 20–30 min and spun at 4 °C for 10–15 min. This last supernatant was removed and the pellet was allowed to air-dry for 5–10 min. Finally, the DNA pellet was dissolved with 10–30 μl TE buffer (10 mM Tris, 1 mM EDTA,

Author Manuscript Author Manuscript Author Manuscript Author Manuscript

pH 8.0). Standard PCR was performed with sets of primers (see Fig. 3) designed for amplification of different segments from the genomic DNA. 5′ end primers, forward: 5′-GCGCGATCGATTTACTGCTATGAG-3′, reverse: 5′-TGCGAATCATTAAAGTGGGTATCA-3′; 3′ end primers, forward: 5′-TATTCCTTTCACTCGCACTTATTG-3′, reverse: 5′-AATGAGGGATACGGGTTCTTTACG. Flanking primers: forward: 5′-AGAGGAGCGTACTATAACCAGAAG-3′, reverse: 5′-GTCCGACCTTTGCAGACTGT-3′

Total RNA preparation and quantitative Real-Time PCR (qRT-PCR)

Total RNA preparation from adult flies and qRT-PCR were carried out as previously described (Peng and Wu, 2007). Briefly, thirty 1–2 day old adult flies of each genotype were frozen in liquid nitrogen, and ground in a 2-ml homogenizer. Total RNA was extracted with the RNeasy Mini kit (Qiagen, Valencia, CA). An on-column DNase digestion was performed during RNA preparation to remove potential genomic DNA contamination. Reverse transcription was performed using the SuperScript III kit (Invitrogen) with random primers. The qRT-PCR probes detecting different regions of the CG33472 transcript were designed on the Roche Universal Probe library website (www.universalprobelibrary.com), and synthesized by Integrated DNA Technology (Coralville, IA). qRT-PCR amplifications were carried out using Power SYBR Green PCR Master Mixer (Qiagen) on an ABI Prism 7000 machine (Applied Biosystems). For each reaction, a single PCR product was indicated by a characteristic dsDNA dissociation temperature. Triplicates of PCR runs were performed on each of the three independent RNA preparations. The expression level of CG33472 transcripts was first normalized to that of the glyceraldehyde-3-phosphate dehydrogenase (GAPDH) gene in the same RNA preparation, then compared between mutants and wild-type controls.

An independent set of qRT-PCR was performed for ry^{+5}, qvr^{1}, qvr^{2}, and qvr^{3} flies. Total RNA was extracted from adult flies using the TRIzol reagent (ThermoFisher). Five hundred nanograms of extracted RNA was reverse-transcribed and amplified using the iTaq universal SYBR green One-step kit (Bio-Rad) with the following *qvr*-specific primers corresponding to the sequences in exons 4 and 5, respectively (CCGTTATCGGATTTCTAACT and CTTGCAGCGGGCATCAGTCC). The relative *qvr* expression levels were calculated using the double-ΔCt method with GAPDH as a housekeeping reference gene, and normalized to the level of *qvr* mRNA in ry^{+5}. The qRT-PCR experiments were performed in triplicates.

mRNA isolation, cDNA synthesis and Reverse-Transcriptase PCR (RT-PCR)

Total RNA was extracted from approximately 300 male homozygous flies per strain using TRIZOL according to the manufacturer's instructions (InVitrogen-Life Technologies, Mississauga, Ont.). Total RNA was treated with TURBO DNA-free kit (Ambion) to remove any contaminated DNA or mRNA was purified from approximately 250 μg of total RNA using the Oligotex mRNA purification kit (Qiagen Inc., Mississauga, Canada). For each strain, one microliter from each cDNA synthesis reaction was subjected to PCR using the following primer pair, forward: 5′-CAATTCGGTTGGCCAGTAGTA-3′ and reverse: 5′-AAGCCTTCTGTCTTTGGAAGC-3′. The locations of primers are designated as open arrows in Figure 2A and the electrophoresis results are shown in Figure 3B.

Author Manuscript Author Manuscript Author Manuscript Author Manuscript

NMJ Electrophysiology

Third-instar larvae of wandering stage were collected from fly bottle walls, and then immediately immersed in a dissection chamber filled with Ca^{2+}-free HL3 saline (in mM, 70 NaCl, 5 KCl, 20 $MgCl_2$, 10 $NaHCO_3$, 5 trehalose, 115 sucrose, and 5 HEPES, at pH 7.2). The larvae were immobilized with insect pins, and then incised longitudinally on the dorsal midline. The organs were carefully removed with forceps, leaving the ventral ganglion and body-wall muscles intact. Afterwards, the saline was replaced with HL3.1, which contained (in mM) 70 NaCl, 5 KCl, 4 $MgCl_2$, 10 $NaHCO_3$, 5 trehalose, 115 Sucrose, and 5 HEPES, at pH 7.2 (Feng et al., 2004). $[Ca^{2+}]_o$ was set to 0.1mM in the majority of experiments, as specified in the Results. The nerve bundles were severed from the ventral ganglion, and 1–2 of them were picked up and sucked in with a stimulation suction electrode (10 μm opening) that was filled with HL3.1. The stimulation voltage was adjusted to 2–2.5 times the threshold voltage to ensure action potential initiation. Ventral muscles 6, 7, 12, and 13 as well as dorsal muscles 1, 2, 9, and 10 were impaled with intracellular glass microelectrodes filled with 3 M KCl, and excitatory junction potential (EJP) recordings were thus obtained. The resistance of the intracellular glass microelectrodes was about 60 MΩ. A direct current amplifier (model M701microprobe system; WPI, Sarasota, FL) was used to detect the signals.

Immunostaining

Wandering stage 3rd instar larvae were dissected in HL3 saline and immediately placed in 3.7% formaldehyde PBS fixative solution for 20 min. Afterwards, the fixed larval preparations were washed on a shaking stage with PBS containing 0.2% triton-X-100 for 3 times, each lasting 15 min. The washed preparations were then incubated with a blocking agent (3% Bovine serum albumin in PBS) for 30 min. Then the preparations were incubated with anti-horseradish peroxidase (FITC-conjugated, 1:50, Jackson ImmunoResearch) overnight at 4 °C. Fluorescent images were taken on a Leica (Buffalo Grove, IL, USA) upright epifluorescence microscope (model DMRBE) with a 40X lens (NA = 0.7).

Electrophysiological recording of amputated legs

Flies were ether anesthetized and their legs were subsequently amputated. An amputated leg was placed between two paper strips soaked with the physiological solution HL3.1 (see methods above), i.e. a high resistance bridge connection between the two conductive strips. Signals from the two paper strips were picked up with a high-gain DC amplifier (x100).

Results

The *qvr^1* mutation mapped to the CG33472 locus

In an EMS screen for the paraquat-sensitive mutants, we identified *qvr^1*, the first allele of *qvr* mutations (Humphreys et al., 1996). Subsequently, we set out to map the genomic location of *qvr*. Our initial complementation data showed that *qvr* was localized in a genomic region which was deleted in the deficiency lines Df(2R)en-B, Df(2R)en-SFX31and Df(2R)en-A (Humphreys et al., 1996; Wang et al., 2000). These lines were mapped to a

Author Manuscript Author Manuscript Author Manuscript Author Manuscript

large region between intersex (*ix*) and walrus (*wal*), which contain 34 annotated loci (listed in Supplementary Table S1).

To refine the mapping, we utilized a number of deletion lines ($qvr^{P1\text{-}1}$, $qvr^{P1\text{-}4}$, and $qvr^{P43\text{-}2}$, see Supplementary Table S2) derived from re-mobilizing the P elements 17en1 and 17en43 inserted in the region (Humphreys, 1996). Complementation tests of these lines showed that they all failed to complement qvr^{1}. However, as shown in Supplementary Table S2, the $qvr^{P1\text{-}1}$ deletion provided the narrowest candidate region, which was approximately 233 kb (Supplementary Table S2, between *Tapδ* and *Egm* in Table S1). Thereby we narrowed the loci of *qvr* to a region containing only 21 genome annotations (see Table S1 for the list of loci).

We previously reported that $In(2R)vg^{135}$, an inversion mutation, disrupts *qvr* function (Humphreys et al. 1996) since $In(2R)vg^{135}$ failed to complement qvr^{1} (summarized in Supplementary Table S3). One of $In(2R)vg^{135}$'s breakpoints was known to be in the gene *Mdr49* (CG3879, Wu et al., 1991), which is distal to the region shown in Table S1 and thus unlikely to disrupt *qvr*. To localize the other breakpoint, we used inverse PCR (Ochman et al., 1988), with primers against *Mdr49* and sequenced $In(2R)vg^{135}$. We found that the proximal breakpoint of $In(2R)vg^{135}$ fell in the region between *Enhancer of Polycomb* [*E(Pc)*] and *invected* (*inv*) (cf. Table. S1, sequence information not shown), where the *qvr* locus resides.

We performed further complementation tests with P insertion lines near this region, and identified that P element disruptions of CG33472 (originally named as CG30032) failed to complement the leg shaking phenotype of qvr^{1} (Figure 1A and Supplementary Tables S3 and S4). In this complementation study, we independently identified the two P insertion lines that disrupted *qvr* function, EY04063 (hereby termed as qvr^{EY}) and f01257 (qvr^{f01257}). The original EY04063 obtained from the Bloomington Stock Center was homozygous lethal. We performed background cleaning by crossing to CS and the second-site lethality was removed (see also Ruan, 2008). These *qvr* alleles were given the unconventional names sss^{P1} and sss^{P2} in the report by Koh et al. (2008).

Identification of new *qvr* alleles with motor control defects

In addition to the initial qvr^{1}, our EMS mutagenesis yielded two new *qvr* alleles, designated as qvr^{2} and qvr^{3}, both of which failed to complement with $qvr^{1.}$ Additionally, we also generated a series of P-element excision lines, via remobilizing the P-element in qvr^{EY} by crossing with a strain carrying a P-element transposase (*y w;; Δ2-3, Sb/TM6, Ubx*). We examined the excision lines for their ether-induced leg shaking phenotype (Figure 1A). Amongst the resultant excision lines, some retained the shaking phenotype while others did not (Table 1). We refer to the non-shaking lines, including qvr^{rv9} and qvr^{rv7}, as "revertants" ("rv"), as they have phenotypically reverted to normal. We name the shaking lines, including qvr^{ip6}, as "imprecise jumpouts" ("ip"), as they still shake under ether (Figure 1A), suggesting deletion and/or insertion due to imprecise excision of the P element.

We compared these *qvr* alleles under ether anesthesia and found *Shaker*-like, vigorous leg shaking in qvr^{1}, qvr^{2}, qvr^{3}, qvr^{ip6}, and qvr^{EY}, but not in the revertants qvr^{rv7} and qvr^{rv9}

Author Manuscript Author Manuscript Author Manuscript Author Manuscript

(Table 1). Another allele, qvr^{f01257}, which is a P-element insertion allele localized not in coding region but in 3′ UTR, also shook mildly (Figure 1A, Table 1; for localization, see Figure 2).

We also performed assays to measure the climbing abilities of *qvr* flies. In this assay (Figure 1B), we noticed that all the shaking *qvr* alleles including qvr^{1}, qvr^{2}, qvr^{3}, qvr^{f0}, qvr^{ip6}, and qvr^{EY} showed weaker climbing abilities than wild-type controls, whereas the revertants were not different from the wild-type (Figure 1C). Varying degree of deficiency was seen among the shaking alleles in that qvr^{3} and qvr^{EY} appeared to be the most extreme alleles, followed by qvr^{1}. In contrast, qvr^{2} and qvr^{ip6} were relatively mild, closer to wild-type controls, despite their clear shaking phenotypes (Figure 1C and Table 1).

Molecular characterization of new *qvr* alleles

So far most studies on *qvr* were derived from the alleles qvr^{1}, qvr^{EY} and occasionally qvr^{f0} (Wang et al., 2000; Koh et al., 2008; Wang and Wu, 2010; Wu et al., 2010; Dean et al., 2011). qvr^{EY} and qvr^{f01257} are P-insertions in the exon 7 and 3′UTR, respectively, whereas the only point mutation, qvr^{1}, is in the intron between exon 6 and 7 (Figure 2, also reported by Koh et al., 2008). Point mutant alleles in exons are lacking.

Here we describe the molecular lesions of qvr^{2} and qvr^{3}, two novel point mutations with their lesions in exon 6 and 7, respectively, flanking the intron-bearing qvr^{1} (Figure 2). DNA sequencing was performed with qvr^{1}, qvr^{2}, and qvr^{3} to determine the lesion sites. Genomic DNA was extracted from 25 homozygous male flies per strain. Approximately 0.25 μg template DNA was used for PCR with the specified primers and the PCR product was used for sequencing (see Materials and Methods). The mutation site of qvr^{2} converts a glycine residue (GGT) to a serine (AGT) in exon 6. Notably, the exon 6 was predicted to contain a glycosylation site (cf. Koh et al., 2008). The mutation site of qvr^{3}, converting a leucine residue (TTA) to a stop codon (TAA), and the insertion site of the P element EY04063 in qvr^{EY} are both in exon 7. Interestingly, a group of four RNA editing sites have been previously reported within exon 7 (Graveley et al., 2011), only 25 base pairs downstream from qvr^{3} (Figure 2B). Further downstream resides the asparagine residue predicted as GPI attachment site (cf. Koh et al., 2008). With these different natures of lesion, it is not surprising that qvr^{1}, qvr^{2} and qvr^{3} confer rather different impacts on *qvr* expression. It was found that qvr^{1} has 3 pieces of mRNA (Figure 3B, cf. Koh et al., 2008), whereas both qvr^{2} and qvr^{3} only have wild type-sized mRNA (Figure 3B).

In addition to the new point mutations, we also generated a series of excision lines from qvr^{EY}, including qvr^{rv9}, qvr^{rv7}, and qvr^{ip6}, by remobilizing the P element EY04063 (see Materials and Methods). In order to verify that the excision had taken place, two sets of PCR primers were designed to test the existence of the P element EY04063 in the genome (see Figure 2A inset for primer localization, see Figure 3A for PCR results). The 5′ primer set flanked exon 5 and the left end of EY04063, and the 3′ primer set flanked right end of the P element EY04063 and part of 3′ UTR. With the EY04063 remaining in the genome, qvr^{EY} mutant flies showed PCR product bands for both 5′ and 3′ primer sets (Figure 3A, left column). Successful excision of the P element will remove the primers within the P element,

Author Manuscript Author Manuscript Author Manuscript Author Manuscript

disrupting either or both of 5′ and 3′ primers. Thus the excision lines including *qvr*^{rv9}, *qvr*^{rv7}, and *qvr*^{ip6} all lost 5′ and 3′ PCR products (Figure 3A).

In addition to 5′ and 3′ primer sets, we had another set of primers named "F" which flanked the 5th, 6th and 7th exons as well as the P element insertion site. Excessive or unclean removal of the P element insertion will alter the sequence length flanked by "F", changing the size of its PCR product. Our PCR results showed that the revertants (*qvr*^{rv9} and *qvr*^{rv7}, which lost leg-shaking phenotype) had consistent-sized "F" PCR products (Figure 3A), which indicates that they are both clean jump-outs, with the P element precisely removed from the genome. This was also supported by reverse-transcriptase PCR results, where wild-type control and *qvr*^{rv7} had similar-sized cDNA (Figure 3B). Unlike the revertant lines, the "F" product of *qvr*^{ip6} was larger than the others, suggesting that it had an incomplete removal of the P element (Figure 3A). The band was undetectable in *qvr*^{EY} (Figure 3B). Consistently, the *qvr* mRNA level in *qvr*^{EY} was also drastically reduced (qRT-PCR results, Figure 3C). This is also in line with the previous Western blot results (Koh et al., 2008). *qvr*^{ip6} reduced the level of mRNA expression as *qvr*^{EY} did, whereas *qvr*^{1} showed enhanced mRNA expression with mRNA products of three different sizes (Figure 3B, see also Koh et. al., 2008). The exon-bearing *qvr*^{2} mutation did not affect the mRNA level, whereas *qvr*^{3} enhanced the mRNA expression (Figure 3C). As all these alleles possess different lesion natures and expression patterns, characterization of their electrophysiological properties may provide helpful information about their usage in future studies.

Differential activity-dependent plasticity of EJP amplitudes in *qvr* alleles

Our previous voltage clamp studies have revealed that *qvr* mutations specifically reduce Shaker-dependent K^+ current I_A in larval muscle (Wang et al, 2000). It was also found that in low-Ca^{2+} saline, *qvr*^{1} mutant displays activity-dependent enhancement in EJCs at unusually low stimulus frequencies (0.1–1.0 Hz, 0.1 mM Ca^{2+}, Wang and Wu, 2010), whereas wild-type NMJs show activity-dependent enhancement only at much higher stimulus frequencies (above 10 Hz, Ueda and Wu, 2006; Wang and Wu, 2010). To uncover any potential novel EJP phenotypes in these new *qvr* alleles, we examined their EJPs with prolonged, repetitive stimulation in 0.1 mM Ca^{2+} saline. For comparison, EJPs from both wild type and *Sh* mutants were collected under the same conditions, with stimulus frequency ranging from 0.2 to 20 Hz.

We observed among the *qvr* alleles the characteristic activity-dependent EJP enhancement, i.e., augmentation, at a low stimulus frequency (0.2 Hz), with the exception of revertants *qvr*^{rv7} and *qvr*^{rv9}, and the 3′ UTR insertion line *qvr*^{f01257} (Figure 4). Consistently, similar augmentation was observed in ventral muscles 6, 7, 14 and dorsal muscles 1, 2, 9 and 10 of these *qvr* mutant alleles (see Figure 4 for data of ventral muscles).

Compared to augmented *qvr* EJPs, wild-type EJPs in 0.1 mM Ca^{2+} saline only displayed quantal fluctuation with a substantial failure rate (70 ± 24%, n = 7), and showed no trend of transmission enhancement even at 0.5 Hz (Figure 4A1, B1, and C, for wild type, 1st EJP amplitude mean ± SD = 0.80 ± 0.95 mV, steady-state = 0.65 ± 0.61 mV). Activity-dependent enhancement of wild-type EJPs required stimulation at a much higher frequency (20 Hz,

Author Manuscript Author Manuscript Author Manuscript Author Manuscript

Figure 4A, right, see Ueda and Wu, 2006 for 10 Hz). Furthermore, at higher stimulation frequencies (5–20 Hz), *qvr* alleles reached the half-augmented plateau level in a far shorter duration than wild type (e.g. qvr^{1}, 1–3 s at 5 Hz, n = 10; qvr^{EY} 0.5–1 s at 5 Hz, n = 8; qvr^{1} and qvr^{3}, 0.5–1 s at 15 Hz, n = 5 vs WT 5–30 s at 10 Hz, n = 5, 10–20 s at 20 Hz, n = 3, see also Figure 4A1 and A2).

Unlike *qvr* and wild type, *Sh* exhibited greatly increased EJP amplitudes without prior stimulus conditioning, but little augmentation upon repetitive stimulation. In other words, *Sh* EJPs did not vary substantially from the very beginning to the end of stimulus trains of both low and high frequencies (Figure 4A1 and A2). It should be noted that such striking differences in the use-dependent EJP phenotype among *qvr*, *Sh* and wild type were best observed at low-Ca^{2+} levels (0.1–0.2 mM) where augmentation is prominent. At increased Ca^{2+} concentrations (e.g. 0.5 mM), the distinctions tended to diminish, as the EJP size approaching saturation levels (Jan et al., 1977; Ueda and Wu, 2006).

Apart from the impressive low-frequency (0.2 Hz) use-dependent augmentation that is about 50–100 times different from wild type (10–20 Hz), *qvr* alleles also displayed defects in the amplitudes of unconditioned (1^{st}) EJPs, which were significantly larger than the WT level but smaller than those of *Sh* alleles (Figure 4C). Notably, distinct from WT, transmission failures rarely occurred in the shaking *qvr* alleles (except for qvr^{f01257}). Among all the *qvr* alleles, qvr^{EY} was most extreme in the unconditioned EJP size. These alterations to different extents, together with the unique low-frequency use-dependent enhancement, all support a critical role of *qvr* in regulating neuromuscular excitability and plasticity.

Mild synaptic overgrowth in *qvr* alleles

It has been shown that neuromuscular hyperexcitability often resulted in increased ramification of the larval neuromuscular junction (Budnik et al., 1990; Zhong et al., 1992). We examined whether the enhanced transmitter release is correlated with overgrowth of larval neuromuscular junctions in *qvr* mutant alleles. We performed immunostaining with FITC-conjugated anti-horse radish peroxidase so as to reveal the mutational effect on NMJ morphology. Both Canton-S and qvr^{rv7} were used as controls. We found that the type Ib boutons of qvr^{EY} allele stood out to be significantly different from wild-type controls in both muscle 12 and 13. Although qvr^{ip6} and qvr^{1} displayed some overgrowth compared to Canton-S, they did not appear to be statistically significantly different from qvr^{rv7} (Figure 5). In general, morphological differences between wild type and *qvr* alleles were small in contrast to the dramatically enhanced synaptic transmission (Figure 5). However, this relatively mild synaptic overgrowth is still surprising when considering the NMJ morphology of *Sh* mutants, which do not exhibit significant synaptic morphology change even in extreme *Sh* alleles (Sh^{120}, Sh^{133}, Budnik et al., 1990; Zhong et al., 1992).

Discussion

In this paper, we review the history of the discovery and characterization of *qvr* mutants and clarify the nomenclature for naming the *qvr* gene. We also present a collection of novel *qvr* alleles, which display varying degree of defects and diverse phenotypes in climbing abilities, leg shaking, synaptic transmission and nerve terminal growth. Together with the original

Author Manuscript Author Manuscript Author Manuscript Author Manuscript

discovery that *qvr* exhibits paraquat sensitivity and defective I_A K^+ channel function (Humphrey et al., 1996; Wang et al., 2000), our results suggest that *qvr* may be implicated in wide-ranging processes, causing defects far beyond "sleepless" (Koh et al., 2008).

Molecular characteristics of *qvr* alleles

In contrast to qvr^1 whose lesion site is in the intron between exons 6 and 7, the point-mutation site of qvr^2 resides in exon 6, whereas qvr^3, qvr^{EY} and qvr^{ip6} were localized in exon 7 (Figure 2). Although all these *qvr* alleles displayed similar ether-induced leg shaking, they demonstrated certain allele-specific preferential effects on the phenotypes examined in this study. For example, qvr^{EY}, i.e. the null allele "*sleepless*" (Koh et al., 2008), displayed the most extreme EJP phenotype (Figure 4) and NMJ overgrowth (Figure 5), but the climbing defect was most extreme in flies with the point-mutation qvr^3 (Figure 2). In addition, the classical allele qvr^1 showed uniformly extreme phenotypes in our characterizations (Figures 1, 3, 4 and 5).

Based on DNA sequencing, exon 7 contains a GPI anchor (Figure 2B). Therefore, exon 7 is potentially important for the membrane localization of Qvr and its interaction with other membrane proteins (Figure 2, GPI anchor and glycosylation sites in the DNA sequence shown here correspond to the locations in the amino acid sequence reported by Koh et al., 2008). Point mutation in exon 7 (qvr^3, see Figure 2) enhanced *qvr* mRNA expression whereas that in exon 6 (qvr^2) did not (Figure 3C). Further, the exon 7 has been reported to have 6 RNA adenosine (A) to inosine (I) editing sites, with 4 resulting in amino acid changes (Graveley et al., 2011, as shown in Figure 2B), not far from the upstream qvr^3, qvr^{EY}, and qvr^{ip6} mutation sites, as well as the predicted GPI anchor attachment site (Figure 2B). RNA editing usually occurs in more conserved exons (Bass and Weintraub, 1988; Jepson and Reenan, 2007; Graveley et al., 2011), and has been previously reported to regulate ion channel excitability in humans, cephalopods as well as *Drosophila* (Bhalla et al., 2004; Garrett and Rosenthal, 2012; Ryan et al., 2012). Therefore, high probability of functional modification by our novel *qvr* alleles, especially those in exon 7, are potentially valuable for further characterization of *qvr* molecular function.

A variety of physiological and behavioral phenotypes potentially conferred by Qvr modulation of Shaker and other interaction partners

As interaction partners, *qvr* and *Sh* share similar behavioral and electrophysiological phenotypes. The mutant qvr^{EY} is especially known for its hyperactivity day and night, and hence named "*sleepless*" (Koh et al., 2008; formally could be named $qvr^{sleepless}$ *or* qvr^{sss}). In fact, not only *qvr*, but also *Sh*, the well-known K^+ channel mutant, has been reported to display "reduced sleep" (Cirelli et al., 2005) albeit below the level of qvr^{EY} (Koh et al., 2008).

Other than defects in circadian locomotive activity, more basic and pervasive phenotypes in both *Sh* and *qvr* are the ether-induced leg shaking (Figure 1 and Table 1) and impaired type I_A K^+ current (Wang et al., 2000; Wu et al., 2010; Wang and Wu, 2010; Dean et al., 2011). However, the characteristic activity and frequency-dependent enhancement of EJP amplitudes in each of the *qvr* mutants available (see also Wang et al., 2000) are distinct from

Author Manuscript Author Manuscript Author Manuscript Author Manuscript

Sh mutations (Figure 4). In addition, *qvr* alleles, especially qvr^{EY}, displayed mild but significant NMJ overgrowth (Figure 5), which was not observed even in extreme *Sh* alleles (Budnik et al., 1990; Zhong et al., 1992). Thus, it is important to note that beyond the clear modulatory role of *qvr* on *Sh* channel operation, some phenotypes studied here might involve the participation of additional proteins. For example, we need to consider interaction through direct physical association, such as Hk as auxiliary beta subunit of Shaker, and the functional interaction between Shaker and Eag (Ganetzky and Wu, 1982 and 1983; Wu et al., 1983; Wu and Ganetzky, 1992) or between Shaker and Shab (Singh and Singh, 1999; Ueda and Wu, 2006; Peng and Wu, 2007).

Considering *qvr* locus itself does not encode an ion channel but a GPI-anchored peptide, it is not surprising that the *qvr* product may have more binding partners than Shaker. In fact, nicotinic acetylcholine receptors (nAChR, Wu et al., 2014, 2016) and GABA transaminase (GABAT, Chen et al., 2015) have been proposed to interact with Qvr. However, these non-Sh interacting partners are mainly expressed in the central nervous system, and are not likely to be involved in *qvr*'s activity-dependent plasticity in NMJ synapses, which are glutamatergic (Jan and Jan, 1976). Therefore, our observations on *qvr* alleles consistently suggest that Shaker is the major interaction partner with Qvr protein to confer the leg-shaking and NMJ-dysfunction phenotypes. To further confirm this idea, we observed that amputated legs from both ether-treated *Sh* and *qvr* flies continue to shake (Ganetzky and Wu, 1985; Figure 6). Spontaneous spiking activities in such isolated peripheral preparation without cholinergic or GABAergic action could be detected using extracellular recording in amputated legs of etherized flies of both *Sh* and *qvr* (Figure 6).

Further investigation with new mutant alleles will be desirable to delineate the functional consequences of Qvr modulation of its interaction with Shaker, nAchR, GABAT, and potentially additional targets.

Supplementary Material

Refer to Web version on PubMed Central for supplementary material.

Acknowledgments

We thank Mr. Anthony McGregor, Mr. Timothy Patience and Dr. Yu Li for assistance in manuscript preparation and proofreading. This work was in part supported by NIH grants NS26528, GM80255, AG047612, and AG051513 (USA), as well as a Natural Sciences and Engineering Research Council Discovery Grant (Canada).

References

Bass BL, Weintraub H. An unwinding activity that covalently modifies its double-stranded RNA substrate. Cell. 1988; 55:1089–1098. [PubMed: 3203381]

Bhalla T, Rosenthal JJ, Holmgren M, Reenan R. Control of human potassium channel inactivation by editing of a small mRNA hairpin. Nat Struct Mol Biol. 2004; 11:950–956. [PubMed: 15361858]

Budnik V, Zhong Y, Wu CF. Morphological plasticity of motor axons in *Drosophila* mutants with altered excitability. J Neurosci. 1990; 10:3754–3768. [PubMed: 1700086]

Chen WF, Maguire S, Sowcik M, Luo W, Koh K, Sehgal A. A neuron-glia interaction involving GABA transaminase contributes to sleep loss in sleepless mutants. Mol Psychiatry. 2015; 20(2):240–51. [PubMed: 24637426]

Author Manuscript Author Manuscript Author Manuscript Author Manuscript

Cirelli C, Bushey D, Hill S, Huber R, Kreber R, Ganetzky B, Tononi G. Reduced sleep in Drosophila Shaker mutants. Nature. 2005; 434(7037):1087–92. [PubMed: 15858564]

Dean T, Xu R, Joiner W, Sehgal A, Hoshi T. *Drosophila* QVR/SSS modulates the activation and C-type inactivation kinetics of *Shaker* K^+ channels. J Neurosci. 2011; 31:11387–11395. [PubMed: 21813698]

Elkins T, Ganetzky B, Wu CF. A *Drosophila* mutation that eliminates a calcium-dependent potassium current. Proc Natl Acad Sci U S A. 1986; 83:8415–8419. [PubMed: 2430288]

Feng Y, Ueda A, Wu CF. A modified minimal hemolymph-like solution, HL3.1, for physiological recordings at the neuromuscular junctions of normal and mutant *Drosophila* larvae. J Neurogenet. 2004; 18:377–402. [PubMed: 15763995]

Ganetzky B, Robertson GA, Wilson GF, Trudeau MC, Titus SA. The *eag* family of K^+ channels in *Drosophila* and mammals. Ann N Y Acad Sci. 1999; 868:356–369. [PubMed: 10414305]

Ganetzky B, Wu CF. *Drosophila* mutants with opposing effects on nerve excitability: Genetic and spatial interactions in repetitive firing. J Neurophysiol. 1982; 47:501–514. [PubMed: 6279790]

Ganetzky B, Wu CF. Neurogenetic analysis of potassium currents in *Drosophila*: Synergistic effects on neuromuscular transmission in double mutants. J Neurogenet. 1983; 1:17–28. [PubMed: 6100303]

Ganetzky B, Wu CF. Genes and membrane excitability in *Drosophila*. Trends in Neurosciences. 1985; 8:322–326.

Garrett SC, Rosenthal JJ. A role for A-to-I RNA editing in temperature adaptation. Physiology. 2012; 27:362–369. [PubMed: 23223630]

Graveley BR, et al. The developmental transcriptome of *Drosophila melanogaster*. Nature. 2011; 471:473–479. [PubMed: 21179090]

Hegde P, Gu GG, Chen D, Free SJ, Singh S. Mutational analysis of the *Shab*-encoded delayed rectifier K^+ channels in *Drosophila*. J Biol Chem. 1999; 274:22109–22113. [PubMed: 10419540]

Hilliker AJ. Genetic analysis of the centromeric heterochromatin of chromosome 2 of *Drosophila melanogaster*: Deficiency mapping of EMS-induced lethal complementation groups. Genetics. 1976; 83:765–782. [PubMed: 823073]

Humphreys JM, Duyf B, Joiner ML, Phillips JP, Hilliker AJ. Genetic analysis of oxygen defense mechanisms in *Drosophila melanogaster* and identification of a novel behavioral mutant with a *Shaker* phenotype. Genome. 1996; 39:749–757. [PubMed: 8776866]

Jan LY, Jan YN. L-glutamate as an excitatory transmitter at the *Drosophila* larval neuromuscular junction. J Physiol. 1976; 262(1):215–36. [PubMed: 186587]

Jan YN, Jan LY, Dennis MJ. Two mutations of synaptic transmission in *Drosophila*. Proc R Soc Lond B Biol Sci. 1977; 198:87–108. [PubMed: 20636]

Jepson JE, Reenan RA. Genetic approaches to studying adenosine-to-inosine RNA editing. Methods Enzymol. 2007; 424:265–287. [PubMed: 17662845]

Kaplan WD, Trout WE 3rd. The behavior of four neurological mutants of *Drosophila*. Genetics. 1969; 61:399–409. [PubMed: 5807804]

Koh K, Joiner WJ, Wu MN, Yue Z, Smith CJ, Sehgal A. Identification of SLEEPLESS, a sleep-promoting factor. Science. 2008; 321:372–376. [PubMed: 18635795]

Komatsu A, Singh S, Rathe P, Wu CF. Mutational and gene dosage analysis of calcium-activated potassium channels in *Drosophila*: Correlation of micro- and macroscopic currents. Neuron. 1990; 4:313–321. [PubMed: 2106331]

Ochman H, Gerber AS, Hartl DL. Genetic applications of an inverse polymerase chain reaction. Genetics. 1988; 120:621–623. [PubMed: 2852134]

Peng IF, Wu CF. *Drosophila cacophony* channels: A major mediator of neuronal Ca^{2+} currents and a trigger for K^+ channel homeostatic regulation. J Neurosci. 2007; 27:1072–1081. [PubMed: 17267561]

Ruan, H. PhD thesis. University of Iowa; 2008. On *Drosophila* aging: Lifespan plasticity, social-behavioral influences, and neurophysiological indices.

Ryan MY, Maloney R, Fineberg JD, Reenan RA, Horn R. RNA editing in *eag* potassium channels: Biophysical consequences of editing a conserved S6 residue. Channels. 2012; 6:443–452. [PubMed: 23064203]

Author Manuscript Author Manuscript Author Manuscript Author Manuscript

Salkoff L, Wyman R. Genetic modification of potassium channels in *Drosophila* shaker mutants. Nature. 1981; 293:228–230. [PubMed: 6268986]

Singh A, Singh S. Unmasking of a novel potassium current in *Drosophila* by a mutation and drugs. J Neurosci. 1999; 19:6838–6843. [PubMed: 10436041]

Singh S, Wu CF. Complete separation of four potassium currents in *Drosophila*. Neuron. 1989; 2:1325–1329. [PubMed: 2516727]

Tsetlin V. Snake venom alpha-neurotoxins and other 'three-finger' proteins. Eur J Biochem. 1999; 264:281–286. [PubMed: 10491072]

Ueda A, Ruan H, Wu CF. The quiver gene encodes a small novel peptide that genetically interacts with several K^+ channel subunits and regulates neuron and muscle excitability in *Drosophila melanogaster*. Society for Neuroscience. 2009; 2009 890.9/GG53.

Ueda A, Wu C-F. Distinct frequency-dependent regulation of nerve terminal excitability and synaptic transmission by IA and IK potassium channels revealed by *Drosophila Shaker* and *Shab* mutations. J Neurosci. 2006; 26(23):6238–48. [PubMed: 16763031]

Wang, JW. PhD thesis. University of Iowa; 1997. Electrophysiological and genetic analyses of *Drosophila* behavioral mutants: the functional roles of voltage-gated potassium channel subunits.

Wang JW, Humphreys JM, Phillips JP, Hilliker AJ, Wu CF. A novel leg-shaking *Drosophila* mutant defective in a voltage-gated K^+ current and hypersensitive to reactive oxygen species. J Neurosci. 2000; 20:5958–5964. [PubMed: 10934243]

Wang Z, Ueda A, Ruan H, Wu CF. Quiver (Sleepless), a new category of K+ channel modulator, affects nerve excitability, synaptic transmission and activity-dependent plasticity. Society for Neuroscience. 2010; 2010 47.3/I2.

Wang JW, Wu CF. Modulation of the frequency response of *Shaker* potassium channels by the *quiver* peptide suggesting a novel extracellular interaction mechanism. J Neurogenet. 2010; 24:67–74. [PubMed: 20429677]

Wu CF, Haugland FN. Voltage clamp analysis of membrane currents in larval muscle fibers of *Drosophila*: Alteration of potassium currents in shaker mutants. J Neurosci. 1985; 5:2626–2640. [PubMed: 2413182]

Wu CF, Ganetzky B. Neurogenetic studies of ion channels in *Drosophila*. Ion Channels. 1992; 3:261–314. [PubMed: 1330057]

Wu CF, Ganetzky B, Haugland FN, Liu AX. Potassium currents in *Drosophila*: Different components affected by mutations of two genes. Science. 1983; 220:1076–1078. [PubMed: 6302847]

Wu CT, Budding M, Griffin MS, Croop JM. Isolation and characterization of Drosophila multidrug resistance gene homologs. Mol Cell Biol. 1991; 11:3940–3948. [PubMed: 2072901]

Wu MN, Joiner WJ, Dean T, Yue Z, Smith CJ, Chen D, Hoshi T, Sehgal A, Koh K. SLEEPLESS, a ly-6/neurotoxin family member, regulates the levels, localization and activity of Shaker. Nat Neurosci. 2010; 13:69–75. [PubMed: 20010822]

Wu M, Liu CZ, Joiner WJ. Structural Analysis and Deletion Mutagenesis Define Regions of QUIVER/SLEEPLESS that Are Responsible for Interactions with Shaker-Type Potassium Channels and Nicotinic Acetylcholine Receptors. PLoS One. 2016; 11(2):e0148215. [PubMed: 26828958]

Wu M, Robinson JE, Joiner WJ. SLEEPLESS Is a Bifunctional Regulator of Excitability and Cholinergic Synaptic Transmission. Current Biology. 2014; 24:621–629. [PubMed: 24613312]

Xing X, Ruan H, Wan X, Ueda A, Wu CF. Quiver/SLEEPLESS, a putative K channel modulator, affects neuromuscular excitability and growth in *Drosophila*. Society for Neuroscience. 2011; 2011 140.07/D56.

Zhong Y, Budnik V, Wu CF. Synaptic plasticity in *Drosophila* memory and hyperexcitable mutants: Role of cAMP cascade. J Neurosci. 1992; 12:644–651. [PubMed: 1371316]

Author Manuscript Author Manuscript Author Manuscript Author Manuscript

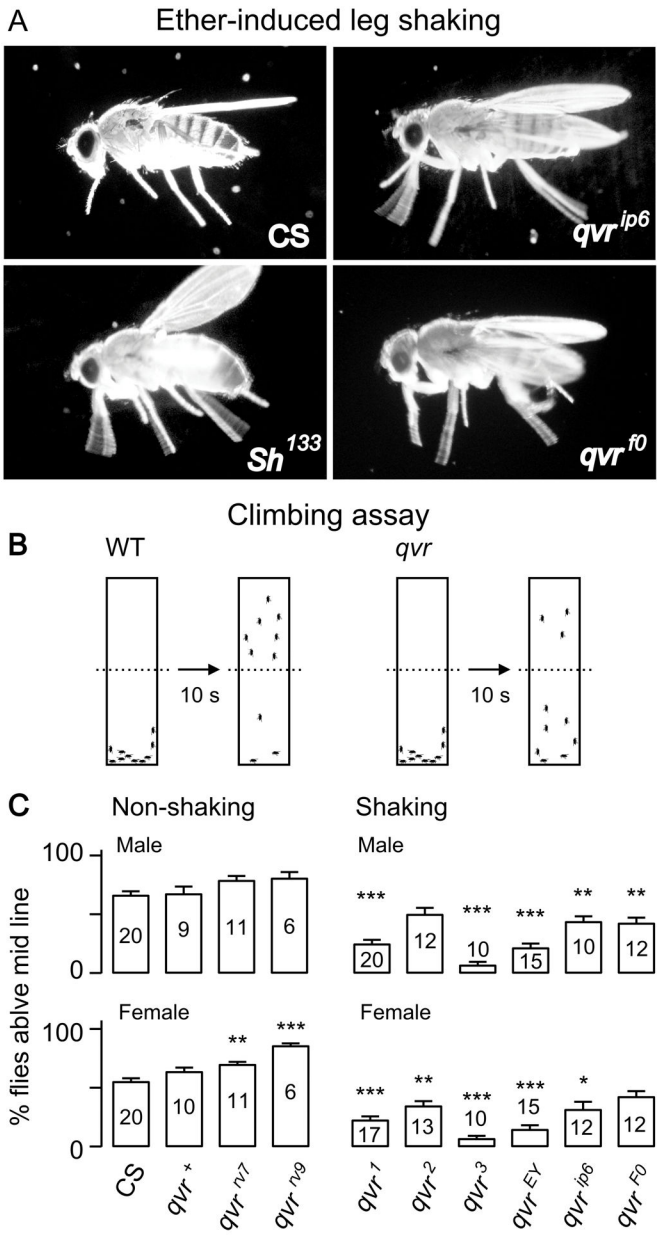

Figure 1. Abnormal motor behaviors in *qvr* and *Sh* flies

(A) Ether-induced leg shaking in *qvr* and *Sh* flies. qvr^{ip6} displayed vigorous leg-shaking similar to Sh^{133}, but qvr^{f0} allele showed only mild shaking. WT (CS) flies do not shake. Dark field photo micrograph, 50-ms exposure. **(B, C)** Weakened climbing ability in *qvr* flies. Number of replicates indicated in (C). 10 flies per trial, see methods. ***, **, and * indicate $p < 0.001$, 0.01, and 0.05 in comparison with CS in t-test with sequential Bonferroni adjustment for multiple comparisons. Error bars indicate SEMs.

Author Manuscript Author Manuscript Author Manuscript Author Manuscript

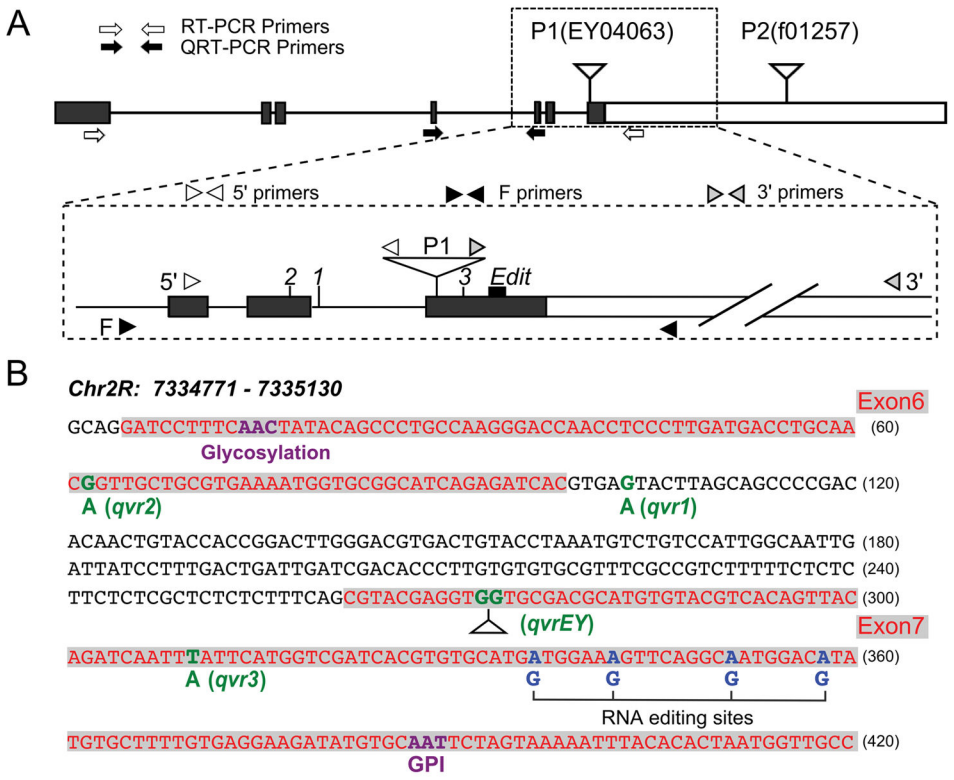

Figure 2. Exon and sequence information of *qvr* alleles

(A) Exons and lesion sites of *qvr* locus. Locations of PCR primers, P1(EY04063) and P2(f01257) insertions are indicated. Open and filled arrows indicate the positions of the primer sets for RT-PCR and qRT-PCR shown in Figure 3B and 3C, respectively. Enlarged box: zoom-in view of exon 5, 6, 7 and part of 3′ untranslated region. Arrow heads indicate locations of the 5′, 3′, and flanking (F) primer sets used in Figure 3A. **(B)** The DNA sequence information for exons 6 and 7, with lesion sites of qvr^{1}, qvr^{2}, qvr^{3}, and qvr^{EY} indicated. Glycosylation, GPI anchor, and RNA-editing sites are also indicated.

Author Manuscript Author Manuscript Author Manuscript Author Manuscript

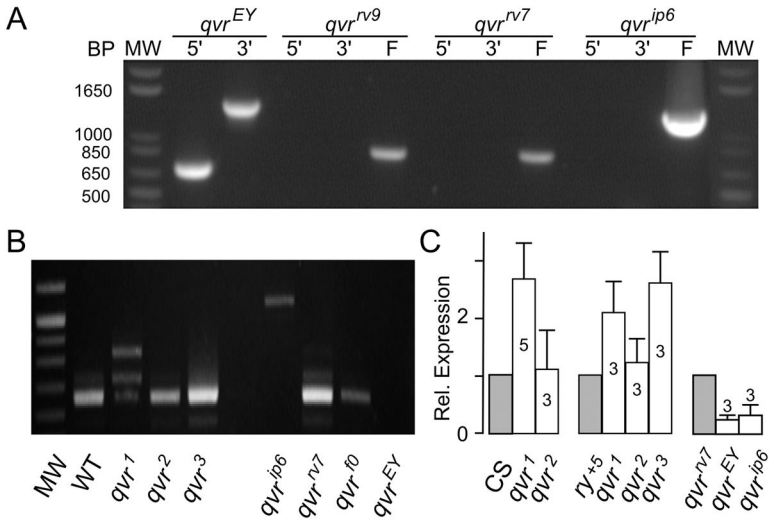

Figure 3. Molecular characterization of *qvr* alleles

(A) Genomic PCR analysis for qvr^{EY} and jumpout lines. The locations of 5′ end, 3′ end and flanking (F) primers are indicated in Figure 2A. **(B)** Reverse-transcriptase PCR results of different *qvr* alleles. Note 3 bands in qvr^{1} but a single band in qvr^{2} and qvr^{3}. **(C)** qRT-PCR studies show the overexpression of *qvr* PCR product in qvr^{1}, unaltered expression level in qvr^{2}, increased expression in qvr^{3}, and decreased expression in qvr^{EY} as well as qvr^{ip6}. Three independent sets of experiments were done, with controls using CS, ry^{+5}, and qvr^{rv7}, respectively. Mutant data were normalized to controls. Number of replicates indicated. For the primers used in (B) and (C), see Figure 2A and Method.

Author Manuscript Author Manuscript Author Manuscript Author Manuscript

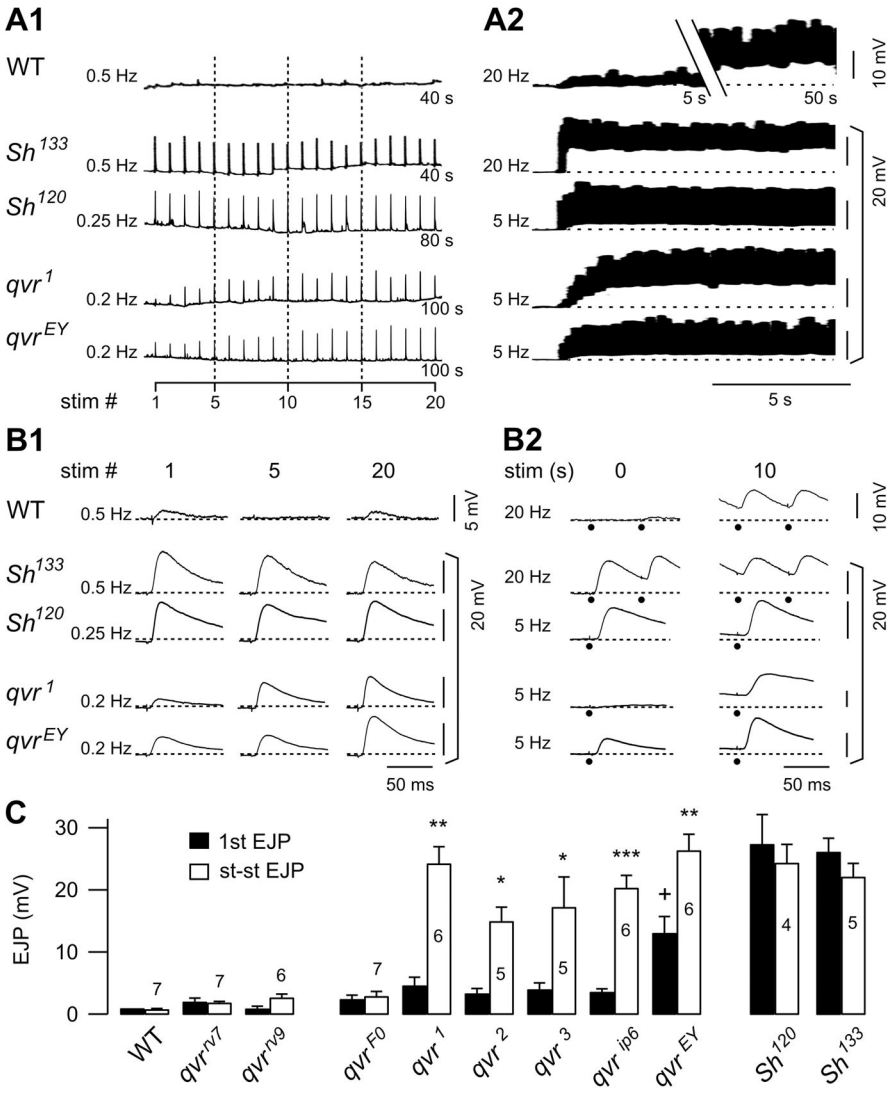

Figure 4. Low-frequency use-dependent enhancement of transmitter release in *qvr* alleles

(**A1 and A2**) Representative EJP recordings over prolonged low-frequency (0.2–0.5 Hz) repetitive stimulation (A1) and high frequency (5–20 Hz, A2) for WT (CS), *Sh*^{133}, *Sh*^{120}, *qvr*^{1} and *qvr*^{EY} (0.1 mM Ca^{2+}). Recording durations and stimulus numbers are indicated in A1. Note the gradual augmentation rising to a plateau-like, steady-state level in *qvr* EJPs with both low (0.2 Hz) and higher frequency (5 Hz) of repetitive stimulation, whereas augmentation in WT occurred only after prolonged high-frequency (20 Hz) stimulation, toward the last 5 s of the 50-s stimulus train as shown in A2. The A2 display is a scanned reproduction of chart recorder traces with a limited temporal resolution of about 0.3 s. **(B1 and B2)** Expanded individual EJPs evoked at 1st, 5th, and 20th stimuli at 0.2–0.5 Hz (B1) and at the initial (0th) and 10th seconds of 5–20 Hz (B2) repetitive stimulation. Same data sets correspond to that shown in A1 and A2, respectively. Note that WT EJPs only displayed quantal fluctuations in response to low-frequency stimulation (0.5 Hz), and that *qvr*^{EY} showed the greatest 1st EJP among *qvr* alleles. **(C)** Summary statistics of 1st EJP (i.e. without prior stimulation, filled bars) and steady-state EJP (st-st EJP, open bars), measured

Author Manuscript Author Manuscript Author Manuscript Author Manuscript

from responses to low-frequency (0.2–0.5 Hz) repetitive stimulation of the indicated genotypes (see A1 traces for example). Significant differences between the 1st and st-st EJPs were found in *qvr* alleles (*, $p < 0.05$; **, $p < 0.01$; ***, $p < 0.001$, paired Students' t-tests with Bonferroni correction), but not in WT, *Sh* alleles, *qvr* revertants (qvr^{rv7} and qvr^{rv9}), and qvr^{f01257} (qvr^{F0}). Among all *qvr* alleles, qvr^{EY} displayed the greatest 1st EJP (+, $p < 0.05$, one-way ANOVA). Error bars indicate SEMs.

Author Manuscript Author Manuscript Author Manuscript Author Manuscript

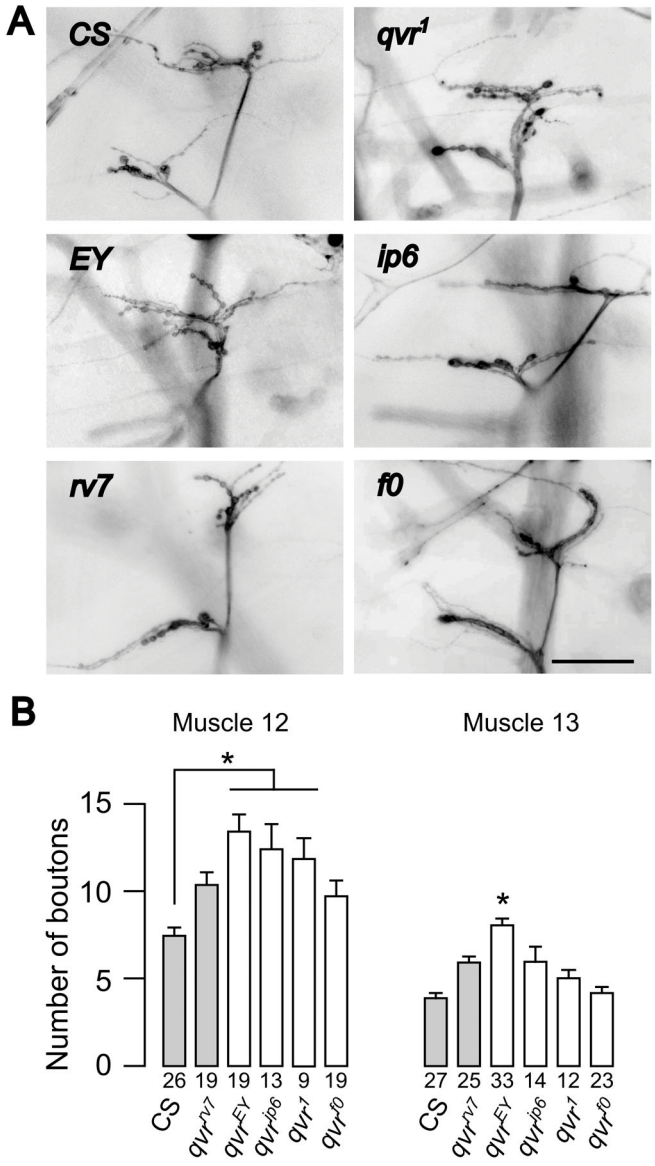

Figure 5. Mild synaptic overgrowth in *qvr* alleles

(A) Sample images of anti-HRP immunostaining of NMJs in muscle 12 and 13 of 3rd instar larvae. Scale bar: 50 μm. **(B)** Type Ib bouton counts for muscle 12 and 13 NMJs. Filled bars indicate control lines. One way ANOVA and Tukey HSD tests were performed. * $p < 0.05$. Error bars indicate SEMs.

Author Manuscript Author Manuscript Author Manuscript Author Manuscript

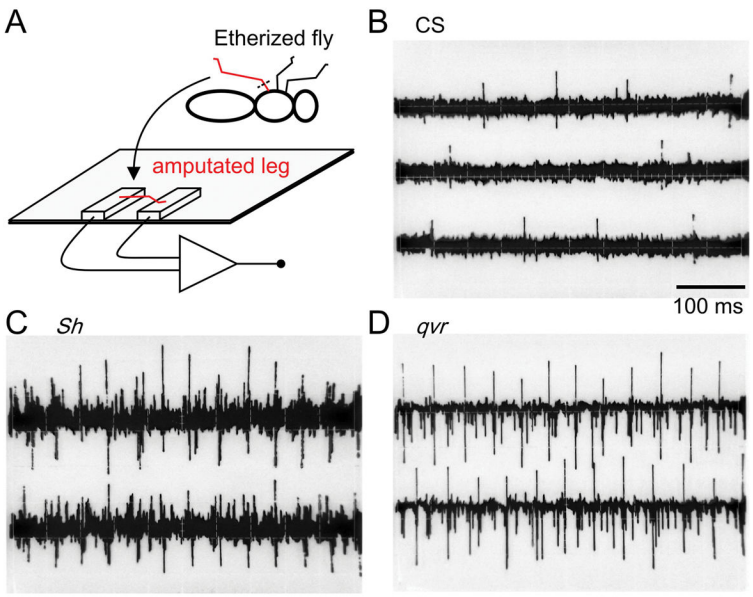

Figure 6. Electrophysiological recordings from amputated legs demonstrating spiking activity correlated with ether-induced shaking

(A) Recording configuration. See Methods for description. (B-D) Representative traces from WT, Sh^{133}, and qvr^{2}. Note the rhythmic firing (~20 Hz) in Sh^{133} and qvr^{2}. Dots indicate action potential spikes.

Author Manuscript Author Manuscript Author Manuscript Author Manuscript

Table 1

List of mutation nature and behavioral phenotypes of all *qvr* alleles.

Genotype	Mutation Location	Molecular Defect	References	Shaking	Motor Coordination **	EJP Amplitude ***	NMJ Growth
Canton-S	Wild type	N.A.		−	Normal	+	+
qvr^{1}	Single site mutation in intron between exons 6&7	Overexpression of altered splicing products	2, 3, 5, 7	++	weak	++++	++
qvr^{2}	Single-site missense mutation in exon 6	Minimal change of expression	7	++	weak	+++	No Data
qvr^{3}	Single-site missense mutation in exon 7	Enhanced expression	7	++	weak	+++	No Data
qvr^{EY}	P element insertion in exon 7	Severely decreased expression	3, 4, 6, 7	++	weak	++++	+++
qvr^{ip6}	Imprecise excision of P element in exon 7	Severely decreased expression	7	++	weak	++++	++
qvr^{rv7}	Precise excision of P element in exon 7	Not applicable	7	−	normal	+	++
qvr^{rv9}	Precise excision of P element in exon 7	Not applicable	7	−	normal	No Data	No Data
qvr^{f01257}	P element insertion in 3′ UTR	Not determined	3, 7	+	normal	+	++

*References, 1. Humphrey et al., 1996; 2. Wang et al., 2000; 3. Koh et al., 2008; 4. Wu et al., 2010; 5. Wang and Wu, 2010; 6. Dean et al., 2011; 7. This paper.

**Climbing assay (Figure 1B)

***steady state EJP amplitude (Figure 3)